



**Queensland University of Technology**  
Brisbane Australia

This may be the author's version of a work that was submitted/accepted for publication in the following source:

Villa, Tommaso Francesco, Jayaratne, Rohan, Gonzalez, Felipe, & Morawska, Lidia

(2017)

Determination of the vertical profile of particle number concentration adjacent to a motorway using an unmanned aerial vehicle.

*Environmental Pollution*, 230, pp. 134-142.

This file was downloaded from: <https://eprints.qut.edu.au/108764/>

**© Consult author(s) regarding copyright matters**

This work is covered by copyright. Unless the document is being made available under a Creative Commons Licence, you must assume that re-use is limited to personal use and that permission from the copyright owner must be obtained for all other uses. If the document is available under a Creative Commons License (or other specified license) then refer to the Licence for details of permitted re-use. It is a condition of access that users recognise and abide by the legal requirements associated with these rights. If you believe that this work infringes copyright please provide details by email to [qut.copyright@qut.edu.au](mailto:qut.copyright@qut.edu.au)

**Notice:** *Please note that this document may not be the Version of Record (i.e. published version) of the work. Author manuscript versions (as Submitted for peer review or as Accepted for publication after peer review) can be identified by an absence of publisher branding and/or typeset appearance. If there is any doubt, please refer to the published source.*

<https://doi.org/10.1016/j.envpol.2017.06.033>

1     **Determination of the Vertical Profile of Particle Number Concentration**  
2             **Adjacent to a Motorway using an Unmanned Aerial Vehicle**

3

4                     T.F. Villa<sup>1</sup>, E.R. Jayaratne<sup>1</sup>, L.F. Gonzalez<sup>2</sup>, and L. Morawska<sup>1\*</sup>

5

6

7

8     <sup>1</sup> International Laboratory for Air Quality and Health (ILAQH), Queensland University of  
9     Technology (QUT), 2 George St, Brisbane QLD 4000;

10    <sup>2</sup> Australian Research Centre for Aerospace Automation (ARCAA), Queensland University of  
11    Technology (QUT), 2 George St, Brisbane QLD 4000;

12

13    \*Corresponding author contact details:

14    Tel: (617)31382616; Fax: (617)31389079

15    Email: [l.morawska@qut.edu.au](mailto:l.morawska@qut.edu.au)

16

17

## 18 **Abstract**

19 A quantitative assessment of the vertical profile of traffic pollution, specifically particle number  
20 concentration (PNC), in an open space adjacent to a motorway was possible for the first time, to  
21 the knowledge of the authors, using a Unmanned Aerial Vehicle (UAV) system. Until now,  
22 traffic pollution has only been measured at ground level while the vertical distribution, is limited  
23 to studies conducted from buildings or fixed towers and balloons. This new UAV system  
24 demonstrated that the PNC sampled during the period from 10 am to 4 pm, outside the rush  
25 hours with a constant traffic flow, increased from a concentration of  $2 \times 10^4$  p/cm<sup>3</sup> near the  
26 ground up to 10 m, and then sharply decreased attaining a steady value of  $4 \times 10^3$  p/cm<sup>3</sup> beyond a  
27 height of about 40 m. While more comprehensive investigations would be warranted under  
28 different conditions, such as topography and vehicle and fuel type, this finding is of great  
29 significance, given that it demonstrates the impact of traffic emissions on human exposure, but  
30 less so to pollution within the upper part of the boundary layer.

31

32 Keywords: Vertical pollution profiles, particle number above the road, UAV and air quality,  
33 urban air pollution

34

## 35 **1. Introduction**

36 Understanding the dispersion of pollutants emitted from urban traffic is important to better  
37 understand their impacts on human health and the environment, and to model and predict their  
38 characteristics.

39 The particle number concentration (PNC) in the urban background varies between  $10^3$  p/cm<sup>3</sup> and  
40  $10^4$  p/cm<sup>3</sup>, but it is up to an order of magnitude greater in the proximity of busy road, motorways

41 (Morawska et al. 2008). The majority of these particles are in the ultrafine size range, below 0.1  
42  $\mu\text{m}$ . The PNC has been measured as a function of distance from roads and the results have  
43 shown that they are the highest near the roads and decrease rapidly in the first few tens of meters  
44 downwind of the road. In one study carried out from 15 up to 375 m downwind of a motorway, it  
45 was shown that the PNC decreased by 50 % between 15 and around 100-150 m from the road,  
46 when the wind was blowing perpendicular to the road (Hitchins et al. 2000; Zhu et al. 2002).

47 While a number of studies provided assessment of ground based horizontal profile of PNC  
48 (Gramotnev et al. 2003; Gramotnev and Ristovski 2004; Morawska et al. 2008; Morawska et al.  
49 1999; Zhu et al. 2008), both the vertical and horizontal profiles are required for meaningful  
50 dispersion modeling and assessment of the impact of traffic emissions. Studies of particle  
51 concentrations from motor vehicle emissions as a function of altitude near the surface are very  
52 limited (Altstädter et al. 2014; Brady et al. 2016; Imhof et al. 2005; Ma and Yu 2014) and mostly  
53 related to urban street canyon measurements (Hitchins et al. 2002; Kumar et al. 2008; Wu et al.  
54 2002). In such microenvironments, measurements are limited to specific heights and positions  
55 and significantly affected by the microclimates created by the buildings (Dimoudi et al. 2013).

56 The dispersion of gaseous pollutants in urban canyons depends on the rate at which the street  
57 exchanges air vertically, with the above roof level atmosphere, and laterally with connecting  
58 streets (N' Riain et al. 1998). Field measurements (DePaul and Sheih 1985; Qin and Kot 1993;  
59 Xie et al. 2003) have shown increased concentrations of traffic-related pollutants on the leeward  
60 sides of urban canyons and decreasing concentrations with height above the ground, on both  
61 sides of the street. These increased leeward concentrations are due to the accumulation of  
62 pollutants locally advected by the large wind vortex that covers most of the canyon. Minor  
63 pollution hotspots might also be created in small cavities where additional recirculation

64 phenomena can take place (Vardoulakis et al. 2003). In urban canyons, PNCs was showed to  
65 change significantly with height, from a maximum concentration between 1.2 and 2 m at street  
66 level decreasing with height to the highest measuring point, normally on the rooftop of the  
67 building. The decrease in PNCs with height in the upper part of the canyon was attributed to the  
68 removal of particles as a result of air mass exchange between the street canyon and the air above  
69 the buildings, while the reduction in PNC at street level (at 1 m) was proposed to be the result of  
70 dilution and dry, turbulent deposition (Kumar et al. 2008). For examples the PNC was monitored  
71 in an urban canyon in Italy (Marini et al. 2015) at sampling heights of 1.2, 5.4, 12.6, and 14.5 m.  
72 The maximum value of PNC was found at 1.2 m and decreased with height. The vertical PNC  
73 profiles on the leeward side, showed a peak at 5.4 m decreasing toward both the lowest (1.2 m)  
74 and highest (14.5 m) sampling points. Measurements though were limited to a small number of  
75 vertical fixed locations.

76 Permanent air quality roadside stations, somewhere present, are typically located on the  
77 pavement of these busy streets, avenues or intersections, within a few meters from the roadway  
78 and with sampling locations at 1.5 – 3 m height above ground (Kumar et al. 2014). While these  
79 results confirm that PNC decreases with height, the use of a UAV in an urban canyon would  
80 enable a more extensive and reliable measurement of the vertical distribution of traffic generated  
81 pollutants, not just within the canyon but, beyond the height of the tallest building.

82 Measurement of PM<sub>1</sub>, PM<sub>2.5</sub>, PM<sub>10</sub>, carried out from a building next to a busy road in China at  
83 six different fixed heights (2, 8, 19, 30, 59 and 79 m), showed that the concentrations decreased  
84 60%, 62% and 80% between 2 and 79 m above the ground, respectively (Wu et al. 2002).  
85 Another study in Singapore, similarly conducted from different floors of a 40 m building located  
86 30 m from a traffic road identified higher values of PM 2.5 at the midfloors, compared with

87 those collected at the upper and lower floors (Kalaiarasan et al. 2009). A further example showed  
88 that concentrations of fine and ultrafine particles decreased to about 50-60% from ground level  
89 readings, between heights of 0 to 6 m, to full building height 24 to 33 m above the ground  
90 (Hitchins et al. 2002). On the contrary, the PNC profile was proposed to be building-specific as it  
91 did not have a consistent pattern (Quang et al. 2012).

92 To date, no studies have reported PNC within the atmospheric column in an open space, close to  
93 urban arterial roads. However, recent advances in hexacopter unmanned aerial vehicle (UAV)  
94 technology have offered a new opportunity for vertical PNC measurements. UAVs have the  
95 capacity to fly close to the ground and to maintain or change direction as required. Information  
96 on the three-dimensional location of the UAV can be reliably obtained by a GPS datalogger  
97 while flying between fixed waypoints, which are GPS points describing the UAV position in  
98 terms of latitude, longitude and altitude. In this study we customized a commercial hexacopter  
99 UAV as a system to measure the vertical profile of PNC in the proximity of a motorway. Here,  
100 we present the results of this study and illustrate the feasibility of using UAVs in order to make  
101 such measurements. The aim of the study was not only to develop a novel measurement system,  
102 but also to use the data to determine the traffic generated PNC vertical profile associated with a  
103 motorway.

104

## 105 **2. Methods**

106 The PNC vertical profile, adjacent to a motorway was measured by mounting a PNC monitor  
107 onboard a DJI S800 hexacopter UAV. The typical flight path was a vertical ascent and descent  
108 above a fixed position on the ground at a distance of 30 m from the kerb of the road. This  
109 position was the minimum distance from a road permitted under the law governing the flight of

110 UAVs in Australia. Traffic flow rate during the experiments was assessed in real time using a  
111 video camera mounted on a second UAV, a DJI Phantom 3 professional quadcopter. The wind  
112 direction throughout the measurement period was approximately from the road towards the point  
113 of measurement. Wind speed and direction, were continuously monitored in real time with a  
114 fixed Monitor weather station located 20 m further downwind from the position where the  
115 hexacopter UAV system started its vertical flight.

## 116 **2.1. The Measurement Site**

117 The measurements were conducted adjacent to the Gateway Motorway in Tingalpa, Brisbane,  
118 Australia, at coordinate 27 29'25.7"S 153 07'21.9"E, where the motorway consisted of eight-  
119 lanes, four in each of the NW-SE direction (Figure 1). Each lane was 4 m wide and the two  
120 directions of traffic were separated by a central reservation of 8 m width. There were no  
121 buildings near the measurement area which was a flat grass field with scattered bushes and trees.  
122 There was a small residential area with parkland on the eastern upwind side of the Motorway  
123 (Figure 1).

124

## 125 **2.2. UAV platforms**

126 The UAV (Figure S1), which was used to accommodate the PNC measuring monitor, was the  
127 S800 EVO manufactured by DJI (DJI 2014). It measures 800 mm in width and 320 mm in height  
128 and is built with composite materials. The S800 is a hexacopter, includes six propellers and  
129 weighs 3.7 kg with minimum and maximum take-off weights of 6.7 kg and 8 kg, respectively.  
130 The UAV uses a 16000 mAh LiPo 6 cell battery, providing a hovering time of approximately 20  
131 min with no additional payload. The hovering motor power consumption is 800 W, when  
132 operating with the minimum take-off weight. Motors run in conjunction with 38 x 13 cm props,

133 each of 13 g. The minimum height above the ground was set to 5 m, being the permitted safe  
134 value. The maximum height was restricted to 100 m which was within the limit permitted by  
135 Civil Aviation Safety Authority . The UAV telemetry range of 2 km was adequate to cover the  
136 entire range of 5 to 100 m.

137 The UAV was equipped with the DJI Wookong autopilot, allowing it to receive pre-programmed  
138 flight path instructions from the ground station software. This software was installed and used  
139 with a portable laptop computer during the field measurements to allow the hexacopter UAV to  
140 be flown autonomously. The autopilot linked with the ground station software also allowed to  
141 track and check the exact location of the UAV during the flight. The ground station software  
142 enabled the UAV action to be related to a specific waypoint, including hovering time (stationary  
143 waiting, while sampling) and translating speed from one waypoint to the next. For each  
144 programmed flight, the ground station software provided an intuitive and easy to use interface  
145 where autonomous flight paths were planned, saved, and uploaded into the UAV. In addition to  
146 the specific flight paths, the software allowed for continuous, real-time monitoring of the status  
147 of the UAV during operation, along with its longitude, latitude, altitude and waypoint tolerance.

148 GPS data was recorded using AARONIA, a small (L/W/D: 102 x 42 x 21 mm), lightweight (88  
149 g), standalone GPS datalogger mounted onboard the UAV. This GPS was necessary because the  
150 Wookong autopilot does not allow the downloading of GPS data. Flight speeds during this study  
151 were 1.5 and 2 m/s, depending on the flight path used.

152 The second UAV used in this research was the DJI Phantom 3 Professional, a quadcopter  
153 (having four propellers), designed for aerial photography and video recording. It carried a high  
154 resolution camera (Sony EXMOR 1/2.3"; Effective pixels: 12.4 millions) and was smaller than



155 the S800 (wheelbase 350 mm, 1.28kg total weight, including batteries; Figure S2, supplementary  
156 material). Its hovering time was about 23 min.

157 The current Civil Aviation Safety Australia (CASA) regulations restrict the use of small (< 20  
158 kg) unmanned aerial systems (UAS) to visual line-of-sight daylight operation, with a maximum  
159 altitude of 400 ft which is approximately 120 m, and within a radius of 3 nmi outside of an  
160 airport. Small UAS cannot be operated above any person or closer than 30 m of populated areas,  
161 houses and people, and are not permitted for research unless the research institution has been  
162 granted a permit. This is possible if the institution has an experienced UAV pilot who is a radio  
163 controller specialist, has a license for commercial UAV operation, along with appropriate  
164 liability insurance . The Queensland University of Technology (QUT) fulfils this requirement  
165 through its Australian Research Centre for Aerospace Aviation (ARCAA), with two pilots who  
166 are in possession of commercial UAV licenses.

167 The DJI S800 was chosen for this study because it is designed to operate under the 20 kg AUW  
168 class of UAS and so reduces operation costs, and avoids being subjected to the tighter  
169 regulations for larger platforms.

170

## 171 **2.3. Instrumentation**

### 172 **2.3.1.PNC**

173 This study used the Mini Diffusion Size Classifier (DISCmini), developed by the University of  
174 Applied Sciences, Windisch, Switzerland (Fierz et al. 2008). The DISCmini is a portable,  
175 battery-operated monitor which can be used to measure number concentration of particles in the  
176 size range 10-500 nm at a fast time resolution of 1 s (1 Hz). The instrument can measure PNC in  
177 a range from  $5 \cdot 10^2$  to over  $10^6$  p/cm<sup>3</sup>. The instrument operates by electrostatically charging the

178 aerosols using a corona discharge and measuring their total surface charge. The accuracy of the  
179 measurement depends on the particle size distribution and is within  $\pm 10-15\%$ , as determined  
180 against a reference condensation particle counter (CPC). The advantages of using the DISCmini  
181 are its relatively small dimensions (180 x 90 x 40 mm), light weight (640 g, 780 g with the probe  
182 used) and long battery life (up to 8 hrs). Importantly, it can easily be integrated on the UAV.  
183 However, careful positioning of the DISCmini is essential in order to avoid possible issues with  
184 the stability of the UAV.

185

### 186 **2.3.2. Meteorological data**

187 An automatic portable Monitor weather station (Automatic Weather Station, Monitor Sensors  
188 (Aust) Pty Ltd.) was used to measure and log the air temperature, relative humidity, atmospheric  
189 pressure, solar radiation intensity, wind speed and wind direction in real time at intervals of 5 s.

### 190 **2.4. Study design**

191 The measurements were conducted over the three days of 19 February, 30 March and 8 April  
192 2016 (day 1, 2 and 3) all of which were weekdays. Days 1 and 2 were used to optimize the study  
193 design, so different vertical flight paths were tested starting from 20 to 60 m and then from 5 to  
194 60 m. The vertical flightpath design was optimized in order to ensure the safety of flights close to  
195 the ground, and to measure PNC distribution along the selected atmospheric column. On day 3,  
196 the flight path was increased to 100 m still in accordance to the maximum height restriction of  
197 120 m permitted by the Civil Aviation Authority. The optimized design path of 5 to 100 m was  
198 adopted on that day 3, and sampling time was limited to the period of 10 am to 4 pm in order to  
199 avoid the morning and afternoon rush hour traffic, and thus to have a steady and consistent  
200 traffic flow rate.

201 Since the closest permitted approach to the Motorway was 30 m, and the minimum altitude 5 m,  
202 the measurements were conducted adjacent to the Motorway in an area that was relatively free of  
203 trees, as indicated by point A, Figure 1 and Figure S3. This location is where the UAV was  
204 operated in a vertical path, climbing to 60 m or 100 m altitude depending on the pre-programmed  
205 flight plan. Point H in Figure 1 represents the ‘home point’, which in UAV terminology refers to  
206 where it takes off and lands. The base camp, B refers to where the UAV operators and scientists  
207 were stationed. Point C represents the position of the automatic portable Monitor weather station.



208

209 Figure 1: Google Earth Image with locations indicated as follows: A - the UAV vertical flight starting point, B - the  
210 base camp, C - the Monitor weather station, H – “home point” of the UAV.

211

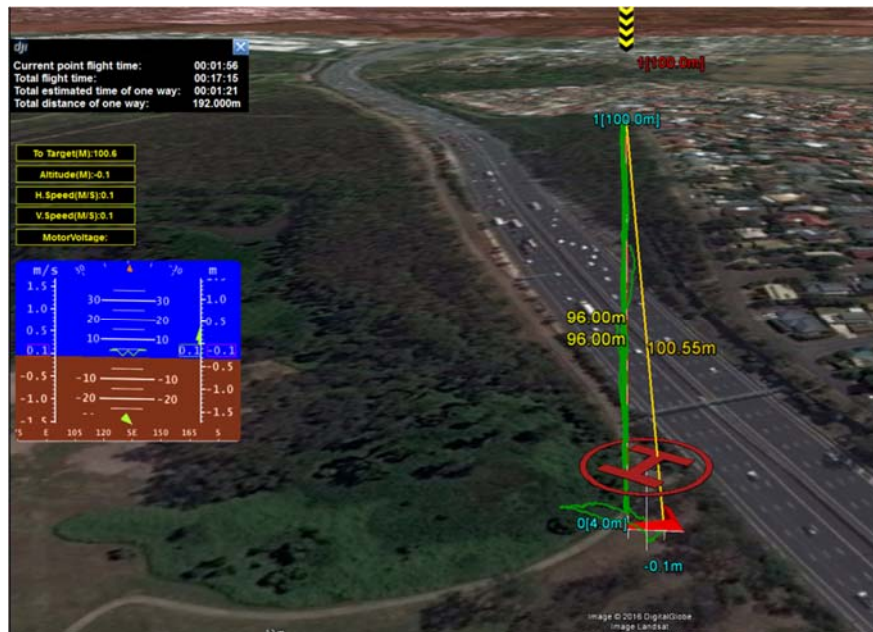
## 212 2.5. Experimental procedure

213 The UAV can fly either manually or autonomously, and as a safety precaution the manual flight  
214 mode was selected for every take-off and landing. Once in the air, the UAV was switched to

215 autonomous flight mode, allowing the platform to follow the pre-programmed flight path of  
216 waypoints.

217 The DISCmini was fitted onboard, underneath the UAV at the beginning of each measuring day  
218 (S1 Figure), and with such payload it could fly for about 12-15 min before landing at the home  
219 point (point H, Figure 1).

220 A typical flight path consisted of a vertical ascent and descent of the atmospheric column,  
221 starting at an altitude of 5 m (above the ground point A, Figure 1) and climbing to 60 m at a  
222 steady speed of  $1.5 \text{ m s}^{-1}$  during days 1 and 2 or up to 100 m at a steady speed of  $2 \text{ m s}^{-1}$  on day 3  
223 Both speeds allowed a significantly continuous number of flights (ascents and descents) before  
224 the battery was exhausted. With each battery, a maximum of 9 ascents and 9 descents were  
225 obtained for the 5 to 100 m flightpath, while a maximum of 14 ascents and 14 descents were  
226 achieved for the shorter flight path from 5 to 60 m. Figure 2 shows a screenshot of the ground  
227 station software, taken from the laptop computer used in field, during a typical 5 to 100 m flight  
228 path. The programmed flights were observed before, during and after its execution. The two  
229 programmed waypoints at 5 and 100 m are also shown together with real time altitude and speed.  
230 Finally, the total flight time and the total estimated time of an ascent plus a descent are shown on  
231 the screen. PNC measurements were taken on the upwind side of the motorway at ground level  
232 just before and after the programmed flights on the downwind side.



233  
234

Figure 2. Screenshot of a typical flight path – a vertical flight from 5 to 100 m

235 The traffic flow rate during the hexacopter UAV vertical flights was determined by the video  
236 footage captured by the camera mounted on the Phantom quadcopter. This UAV was operated  
237 manually by the second ARCAA pilot. It was set to hover at a height of about 60 m above a  
238 point on the ground that was about 40 m away from the kerb of the motorway.

239 At the beginning of each day, all devices, including the weather station, were fully charged,  
240 switched on and were synchronized to the same time with a precision of  $\pm 1$ s. Devices were  
241 switched off only at the completion of all measurements. The onboard devices, DISCmini and  
242 AARONIA data logger were activated to log data simultaneously from take-off to landing. The  
243 logging of data on both devices was terminated at the same time after each flight and data were  
244 downloaded to the computer.

### 245 3. Results

246 The UAV system, with the onboard DISCmini, measured the vertical distribution of PNC,  
247 acquiring data from 34 ascents and 34 descents from near the ground up to an altitude of 60 m

248 during days 1 and 2. Data from 9 ascents and 9 descents from 5 to 100 m were acquired on the  
249 third day using the optimized flight path. There were the data used for the analysis.

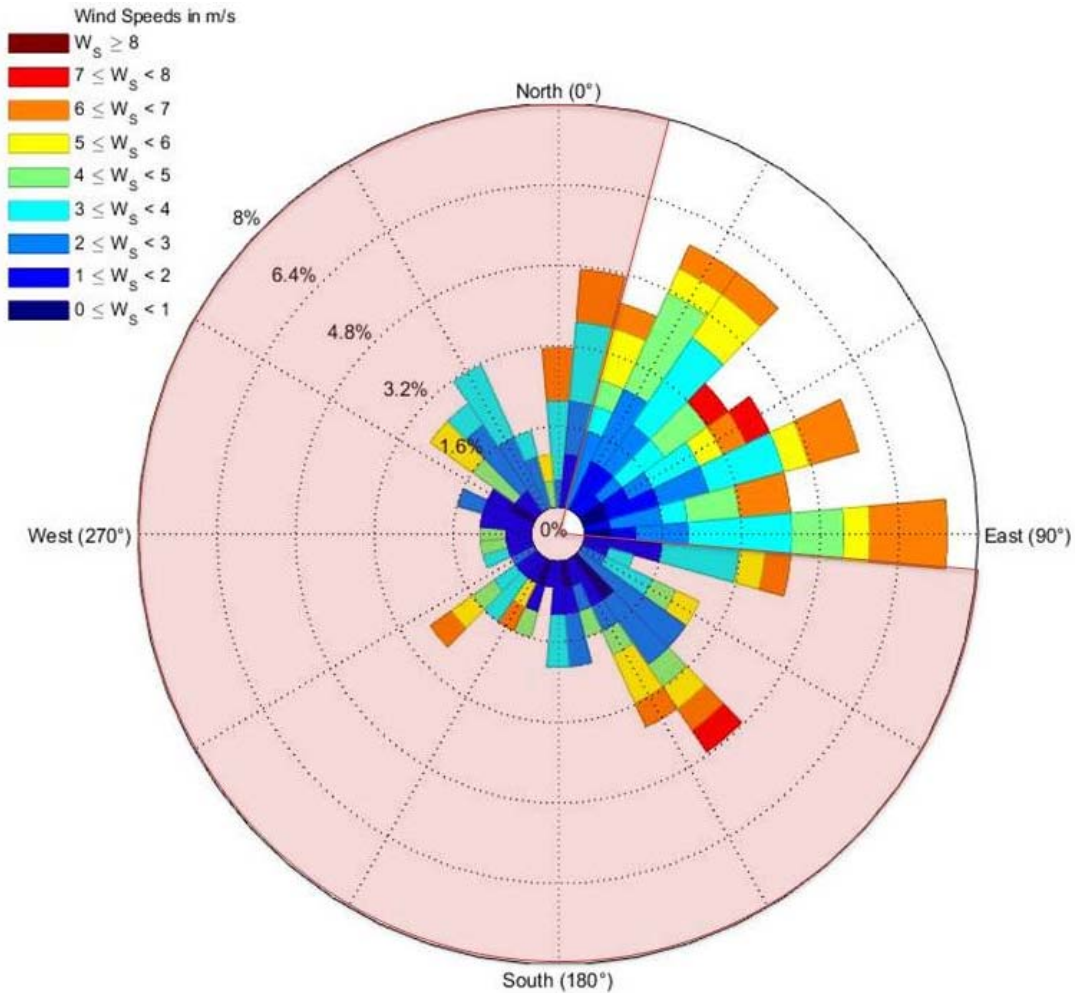
250

### 251 **3.1. Meteorological conditions**

252 Wind conditions, followed two main patterns for most of the time. The wind speed ranged from  
253 3 - 7 m s<sup>-1</sup>. The wind direction was predominantly from the NE or E which corresponded to a  
254 direction from the Motorway towards the adjacent tree-free area where the measurements were  
255 conducted (from the Motorway to point A in Figure 1). Occasionally wind gusts were  
256 experienced during the measurements and they were identified and later considered in the  
257 analysis by the automatic weather station and those from the GPS datalogger.

258 The wind rose graph in Figure 3, illustrates the wind data recorded with the automated weather  
259 station, for the duration of all the 5 to 100 m vertical flights, on day 3. In the case presented, the  
260 prevalent wind direction was from the E and ENE.

261 The wind direction changed occasionally to W and WSW in the opposite direction and when this  
262 happened the pollutants from the motor vehicles were not received at the measurement site and  
263 therefore the data were not usable for our purpose. The shaded section in Figure 3 represents  
264 wind directions which were not suitable for the measurements. As a result, 2 of the 9 complete  
265 flights (ascents and descents) of the 5 to 100 m vertical flight were excluded from the analysis.



266

267 Figure 3 – Wind rose showing wind speed and direction, during the time period of the 5 to 100 m vertical flights.

268

### 269 3.2. Traffic conditions

270 The traffic flow rate during all three days of measurement in the four lanes of the motorway was

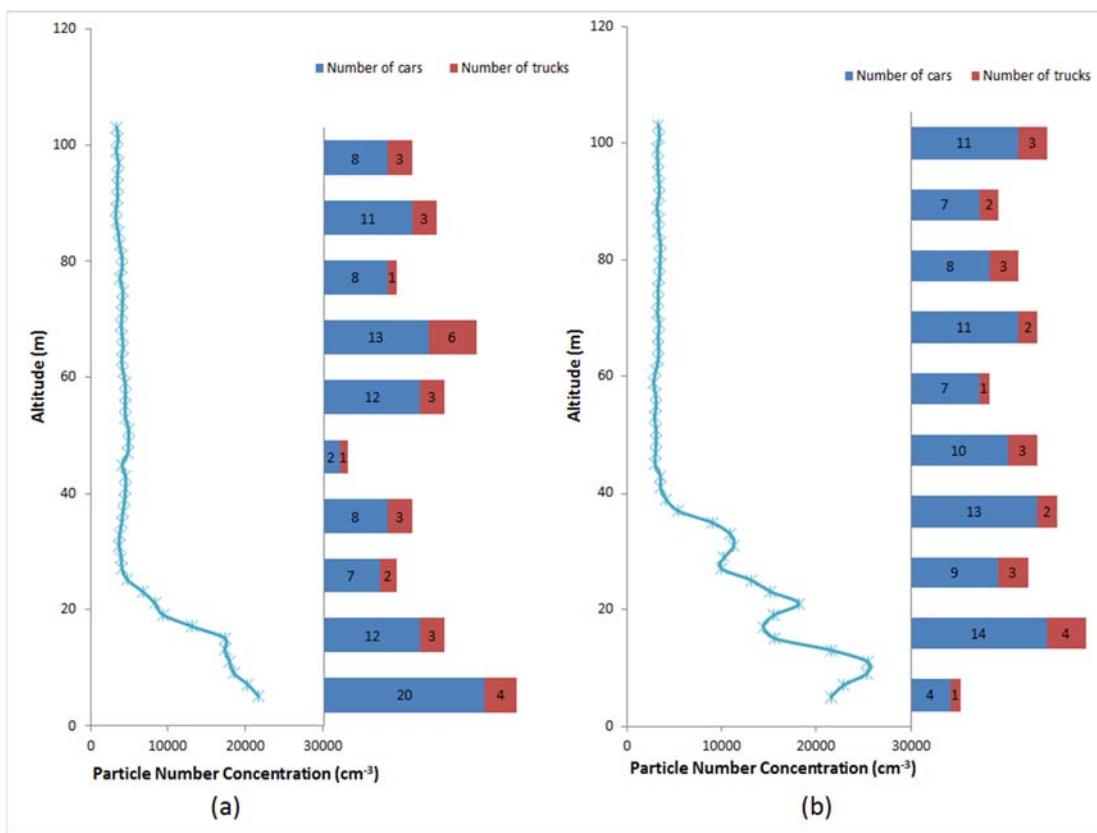
271 in the range of 110-130 vehicles  $\text{min}^{-1}$ , of which about 20% were heavy-duty diesel vehicles.

272 Most traffic moved freely at a steady speed of about 100  $\text{km h}^{-1}$ .

273

### 274 3.3. Ascent and descent measurements

275 Figure 4 (a) and (b) shows the PNC distributions together with the traffic flow rate, of a typical 5  
 276 to 100 m ascent and descent. The graphs in Figure 4 show that the PNC varied by an order of  
 277 magnitude over the entire profile, with the greatest variation being observed closest to the  
 278 ground. The flight presented in Figure 4 (b) shows that the PNC increased up to 10 m from the  
 279 ground before PNC starts to decrease sharply with altitude, within the first 20 m, and then  
 280 decreasing gently. PNC did not vary significantly at heights above 35 m. This unexpected  
 281 pattern, of the PNC increasing up to 10 m, was observed in some ascents and descents. This  
 282 phenomenon will be further discussed in the Discussion.



283

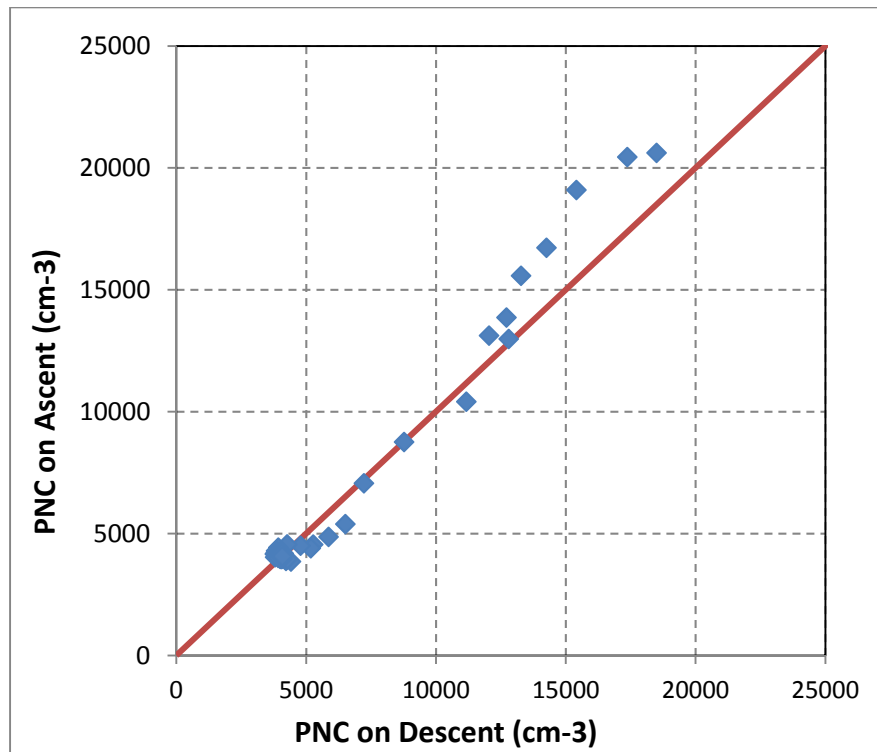
284 Figure 4. Typical PNC profiles (left) and corresponding histogram of the traffic flow rate presented in 5s intervals  
 285 (right) of an ascent (a) and a descent (b) between 5 and 100 m.

286

287 The PNC profiles in the ascents and descents were expected to be similar. To verify, the mean  
 288 PNC was plotted at a given altitude during the ascents against the mean PNC during the descents



289 as shown in Figure 5. At a given altitude there was a good correlation between the PNC  
 290 measured during both the ascents and the descents.



291

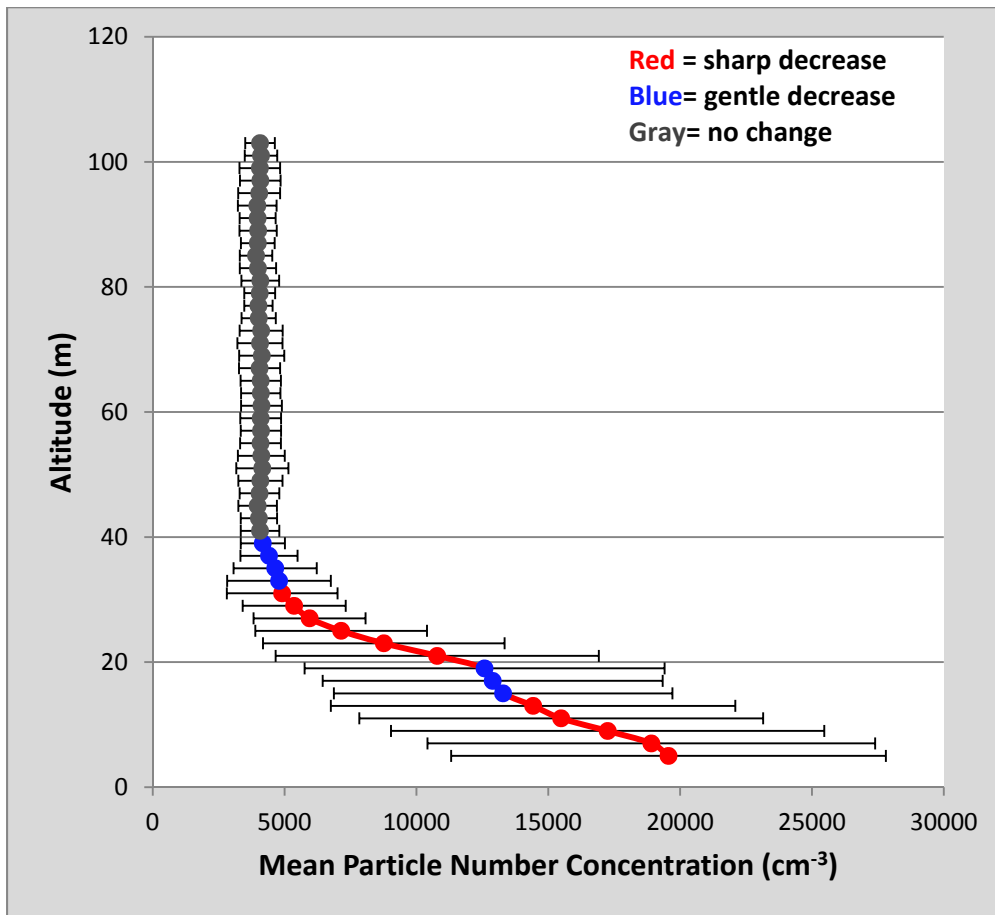
292 Figure 5. Mean PNC of the ascents (Y axe) and descents (X axe) for the flights between 5 and 100 m.

293 Figure S4 (supplementary material) shows the mean, with standard deviations of the PNC  
 294 measured during (a) the seven ascents and (b) seven descents of the 5 to 100 m vertical flights.

295 Figure 6 shows the mean with standard deviations of all 14 PNC vertical profiles of the 5 to 100  
 296 m flight path, consisting of 7 ascents and 7 descents, combined together. The mean PNC  
 297 decreased sharply from 5 m to 15 m, and then decreased very gently up to 18 m. The mean PNC  
 298 then decreased sharply again, and attained the steady value of  $4 \cdot 10^3$  p/cm<sup>3</sup> at about 40 m. The  
 299 mean PNC dropped by an order of magnitude in a height of less than 20 m.

300 Figure S5 (SI) shows the mean with standard deviations of all 24 PNC vertical profiles of the 5  
 301 to 60 m flight paths acquired during days 1 and 2. While these data were not used for the

302 analysis, as they are acquired to optimize the procedure, it can be seen that the trends in the  
 303 vertical profile are the same on day 3.



304  
 305 Figure 6. PNC mean with standard deviation of both seven ascents and seven descents during the 5 to 100 m vertical  
 306 flights.

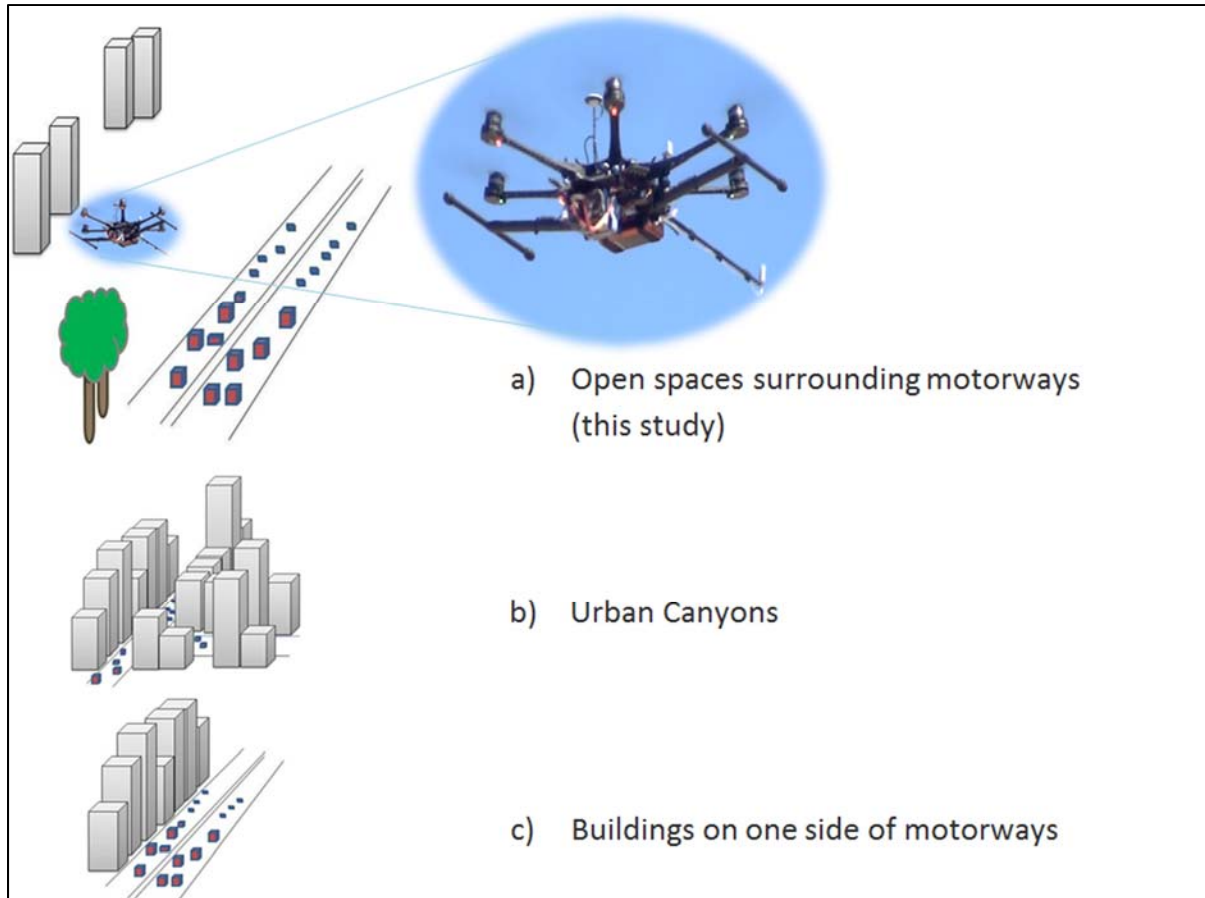
#### 307 4. Discussion

308 This study assessed the vertical distribution of traffic generated pollutants in an open space  
 309 adjacent to a motorway. This was achieved by customizing and flying a hexacopter UAV  
 310 vertically through an atmospheric column (0-100 m). The choice of the DJI Wookong autopilot  
 311 was based on the technical features of the UAV platform. Such autopilot was the most reliable to  
 312 be used with the S800 hexacopter because both autopilot and UAV are produced by DJI. Future  
 313 work will include a focus on other UAV autopilots (Pixhawk) to be integrated with the S800.

314 Different autopilots have serial and analog input connections for further sensor integrations with  
315 the possibility of temperature profile and other atmospheric parameters measured in flight. We  
316 demonstrated the feasibility of a new system, which measures with high spatial and temporal  
317 resolution (time: 1 s; space:  $\pm 0.5$  m) the variation of traffic generated PNC as function of height  
318 in an open space adjacent to a busy motorway, as presented in Figure 7a.

319 The use of this UAV system allowed for the first time, to the knowledge of the authors, to  
320 determine the vertical distribution of PNC, from 5 up to 100 m, continuously. Our study,  
321 established that the PNC in the atmospheric column decreased sharply from 5 m, up to about 15  
322 m before starting to decrease very gently up to 18 m. Then, the PNC decreased sharply again  
323 reaching a steady value after 40 m. The PNC was measured at ground level at the upwind side of  
324 the motorway before and after the downwind measurements and showed readings in the range of  
325 600 – 1000 p/cm<sup>3</sup>. The corresponding ground level PNC readings on the downwind side of  
326 motorway were in the range of 35,000 – 45,000 p/cm<sup>3</sup>, indicating that the large majority of  
327 pollutants originated from motor vehicles travelling on the motorway.

328 This study showed that the traffic generated PNC above the ground (5 m), during the period to  
329 10 am to 4 pm, outside the rush hours, were of the order of  $2 \cdot 10^4$  p/cm<sup>3</sup>, and it attained a steady  
330 value of the order of  $4 \cdot 10^3$  p/cm<sup>3</sup> above a height of 40 m. Therefore our results suggest that  
331 emissions from vehicles on the motorway did not directly affect the environment above this  
332 height. Using this hexacopter UAV system to assess the PNC vertical profile throughout an  
333 atmospheric column, in open spaces adjacent to a traffic motorway, provided knowledge to  
334 improve dispersion models to better protect populations living close to such pollutant sources.  
335 Such measurements were previously not possible with fixed-site measurements at ground level,  
336 or from a distant tall building, and this is a significant finding.



337

338

Figure 7. Schematic representation of urban environments

339

340

341

342

343

344

345

346

347

This study in an open space environment adjacent to a motorway differs from other studies conducted in constrained urban environments, such as in urban canyons (Figure 7 b), which are typically relatively narrow streets with buildings lined up continuously along both sides (Nicholson 1975). Figure 7c presents a different scenario from narrow urban canyons, one where buildings are lined along only one side of a major road. Here, the air travels a sufficient distance downwind of the first building before encountering the next (Vardoulakis et al. 2003). The vertical particle mass concentration profile in such cases largely shows a consistent decrease in concentration with increasing distance from nearby streets (Chan and Kwok 2000; Micallef and Colls 1998; Rubino et al. 1998).

348 In general, all these previous studies have illustrated that both PNC and PM decreased with  
349 altitude next to high rise buildings in street canyons (Vardoulakis et al. 2003). An important  
350 observation made in the present study, which differs from previous ones of both urban canyons  
351 and buildings near traffic roads, is that in some cases the PNC in the vertical plane increases  
352 from the ground up to about 10 m before starting to decrease with height. We attribute this to the  
353 fact that the exhaust tubes of most heavy duty trucks project vertically upwards and are located at  
354 a height of some several meters above ground. A significant proportion of vehicles on the traffic  
355 motorway, from 20 to 30 % of the total traffic count, consisted of heavy-duty diesel trucks. This  
356 is not the case in urban canyons where most of the vehicles were motor cars with the tailpipes  
357 close to street level. Another observation we made, is that the mean PNC values during both the  
358 ascents and descents had very similar patterns as shown in Figure 5. The average PNC for  
359 ascents at a given altitude did not differ significantly to the average PNC at the same point  
360 during the descents. This was the first application, to the knowledge of the authors, of UAV for  
361 the determination of PNC vertical profile of urban air quality; previously UAV systems have  
362 been used to investigate aerosol vertical profiles at the ocean coast (Brady et al. 2016).

363

## 364 **5. Conclusion**

365 In this study we have presented the potential for broader applications of UAV systems in  
366 assessments of the PNC vertical profile. However, it is the strict civil aviation regulation for  
367 UAV deployment that currently limits the use of UAV systems for PNC measurements,  
368 specifically in urban environments.

369 Moreover, this hexacopter UAV system can be utilized in environments where UAV use is less  
370 strict, such as open spaces away from urban centers or to monitor concentrations and dispersion  
371 of plumes emitted by industrial stacks and ships in the ocean.

372

### 373 **Acknowledgements**

374 The authors would like to acknowledge the ARCAA Operations Team (Dirk Lessner, Dean  
375 Gilligan, Gavin Broadbent and Dr Dmitry Bratanov) who operated the Unmanned Aerial Vehicle  
376 (S800).

377 The authors would also like to acknowledge the help of the QUT Academic Language and  
378 Learning Service, in particular Karyn Gonano for the language editing of this manuscript.

### 379 **Appendix A.** Supplementary material

### 380 **References**

- 381 NPRM 1309OS - Remotely Piloted Aircraft Systems.  
382 Altstädter, B.; Platis, A.; Wehner, B.; Scholtz, A.; Lampert, A.; Wildmann, N.; Hermann, M.;  
383 Käthner, R.; Bange, J.; Baars, H. ALADINA—an unmanned research aircraft for  
384 observing vertical and horizontal distributions of ultrafine particles within the  
385 atmospheric boundary layer. *Atmospheric Measurement Techniques Discussions*  
386 2014;7:12283-12322
- 387 Brady, J.M.; Stokes, M.D.; Bonnardel, J.; Bertram, T.H. Characterization of a Quadrotor  
388 Unmanned Aircraft System for Aerosol-Particle-Concentration Measurements.  
389 *Environmental Science & Technology* 2016;50:1376-1383
- 390 Chan, L.Y.; Kwok, W.S. Vertical dispersion of suspended particulates in urban area of Hong  
391 Kong. *Atmospheric Environment* 2000;34:4403-4412
- 392 DePaul, F.T.; Sheih, C.M. A tracer study of dispersion in an urban street canyon. *Atmospheric*  
393 *Environment* (1967) 1985;19:555-559
- 394 Dimoudi, A.; Kantzioura, A.; Zoras, S.; Pallas, C.; Kosmopoulos, P. Investigation of urban  
395 microclimate parameters in an urban center. *Energy and Buildings* 2013;64:1-9
- 396 DJI. DJI S800-evo. 2014
- 397 Fierz, M.; Burtscher, H.; Steigmeier, P.; Kasper, M. Field measurement of particle size and  
398 number concentration with the Diffusion Size Classifier (DiSC). SAE Technical Paper;  
399 2008
- 400 Gramotnev, G.; Brown, R.; Ristovski, Z.; Hitchins, J.; Morawska, L. Determination of average  
401 emission factors for vehicles on a busy road. *Atmospheric Environment* 2003;37:465-474

- 402 Gramotnev, G.; Ristovski, Z. Experimental investigation of ultra-fine particle size distribution  
403 near a busy road. *Atmospheric Environment* 2004;38:1767-1776
- 404 Hitchins, J.; Morawska, L.; Gilbert, D.; Jamriska, M. Dispersion of particles from vehicle  
405 emissions around high- and low-rise buildings. *Indoor Air* 2002;12:64-71
- 406 Hitchins, J.; Morawska, L.; Wolff, R.; Gilbert, D. Concentrations of submicrometre particles  
407 from vehicle emissions near a major road. *Atmospheric Environment* 2000;34:51-59
- 408 Imhof, D.; Weingartner, E.; Vogt, U.; Dreiseidler, A.; Rosenbohm, E.; Scheer, V.; Vogt, R.;  
409 Nielsen, O.J.; Kurtenbach, R.; Corsmeier, U.; Kohler, M.; Baltensperger, U. Vertical  
410 distribution of aerosol particles and NO<sub>x</sub> close to a motorway. *Atmospheric Environment*  
411 2005;39:5710-5721
- 412 Kalaiarasan, M.; Balasubramanian, R.; Cheong, K.W.D.; Tham, K.W. Traffic-generated airborne  
413 particles in naturally ventilated multi-storey residential buildings of Singapore: Vertical  
414 distribution and potential health risks. *Building and Environment* 2009;44:1493-1500
- 415 Kumar, P.; Fennell, P.; Langley, D.; Britter, R. Pseudo-simultaneous measurements for the  
416 vertical variation of coarse, fine and ultrafine particles in an urban street canyon.  
417 *Atmospheric Environment* 2008;42:4304-4319
- 418 Kumar, P.; Morawska, L.; Birmili, W.; Paasonen, P.; Hu, M.; Kulmala, M.; Harrison, R.M.;  
419 Norford, L.; Britter, R. Ultrafine particles in cities. *Environment International* 2014;66:1-  
420 10
- 421 Ma, X.; Yu, F. Seasonal variability of aerosol vertical profiles over east US and west Europe:  
422 GEOS-Chem/APM simulation and comparison with CALIPSO observations.  
423 *Atmospheric Research* 2014;140-141:28-37
- 424 Marini, S.; Buonanno, G.; Stabile, L.; Avino, P. A benchmark for numerical scheme validation  
425 of airborne particle exposure in street canyons. *Environmental Science and Pollution*  
426 *Research* 2015;22:2051-2063
- 427 Micallef, A.; Colls, J.J. Variation in airborne particulate matter concentration over the first three  
428 metres from ground in a street canyon: implications for human exposure. *Atmospheric*  
429 *Environment* 1998;32:3795-3799
- 430 Morawska, L.; Ristovski, Z.; Jayaratne, E.R.; Keogh, D.U.; Ling, X. Ambient nano and ultrafine  
431 particles from motor vehicle emissions: Characteristics, ambient processing and  
432 implications on human exposure. *Atmospheric Environment* 2008;42:8113-8138
- 433 Morawska, L.; Thomas, S.; Gilbert, D.; Greenaway, C.; Rijnders, E. A study of the horizontal  
434 and vertical profile of submicrometer particles in relation to a busy road. *Atmospheric*  
435 *Environment* 1999;33:1261-1274
- 436 N' Riain, C.M.; Fisher, B.; Martin, C.J.; Littler, J. Flow Field and Pollution Dispersion in a  
437 Central London Street. *Environ Monit Assess* 1998;52:299-314
- 438 Nicholson, S.E. A pollution model for street-level air. *Atmospheric Environment* (1967)  
439 1975;9:19-31
- 440 Qin, Y.; Kot, S.C. Dispersion of vehicular emission in street canyons, Guangzhou City, South  
441 China (P.R.C.). *Atmospheric Environment Part B Urban Atmosphere* 1993;27:283-291
- 442 Quang, T.N.; He, C.; Morawska, L.; Knibbs, L.D.; Falk, M. Vertical particle concentration  
443 profiles around urban office buildings. *Atmos Chem Phys* 2012;12:5017-5030
- 444 Rubino, F.M.; Floridia, L.; Tavazzani, M.; Fustinoni, S.; Giampiccolo, R.; Colombi, A. Height  
445 profile of some air quality markers in the urban atmosphere surrounding a 100 m tower  
446 building. *Atmospheric Environment* 1998;32:3569-3580

- 447 Vardoulakis, S.; Fisher, B.E.A.; Pericleous, K.; Gonzalez-Flesca, N. Modelling air quality in  
448 street canyons: a review. *Atmospheric Environment* 2003;37:155-182
- 449 Wu, Y.; Hao, J.; Fu, L.; Wang, Z.; Tang, U. Vertical and horizontal profiles of airborne  
450 particulate matter near major roads in Macao, China. *Atmospheric Environment*  
451 2002;36:4907-4918
- 452 Xie, S.; Zhang, Y.; Qi, L.; Tang, X. Spatial distribution of traffic-related pollutant concentrations  
453 in street canyons. *Atmospheric Environment* 2003;37:3213-3224
- 454 Zhu, Y.; Fung, D.C.; Kennedy, N.; Hinds, W.C.; Eiguren-Fernandez, A. Measurements of  
455 ultrafine particles and other vehicular pollutants inside a mobile exposure system on Los  
456 Angeles freeways. *J Air Waste Manage Assoc* 2008;58:424-434
- 457 Zhu, Y.; Hinds, W.C.; Kim, S.; Shen, S.; Sioutas, C. Study of ultrafine particles near a major  
458 highway with heavy-duty diesel traffic. *Atmospheric Environment* 2002;36:4323-4335
- 459
- 460



461 **Supplementary Material (SM) For:**

462

463 **Determination of the Vertical Profile of Particle Number Concentration Adjacent to a**

464 **Traffic Motorway using an Unmanned Aerial Vehicle**

465

466 T.F. Villa<sup>1</sup>, E.R. Jayaratne<sup>1</sup>, L.F. Gonzalez<sup>2</sup>, and L. Morawska<sup>1\*</sup>

467

468 <sup>1</sup> International Laboratory for Air Quality and Health (ILAQH), Queensland University of  
469 Technology (QUT), 2 George St, Brisbane QLD 4000;

470 <sup>2</sup> Australian Research Centre for Aerospace Automation (ARCAA), Queensland University of  
471 Technology (QUT), 2 George St, Brisbane QLD 4000;

472 \*Corresponding author: l.morawska@qut.edu.au

473

474

475 Pages           6

476

477 Figures          5

478



479

480 **Figure S1:** The UAV system. the DJI S800 UAV with the DISCmini mounted onboard.



481

482 **Figure S2:** S800 hexacopter and the Phantom quadcopter

483

484



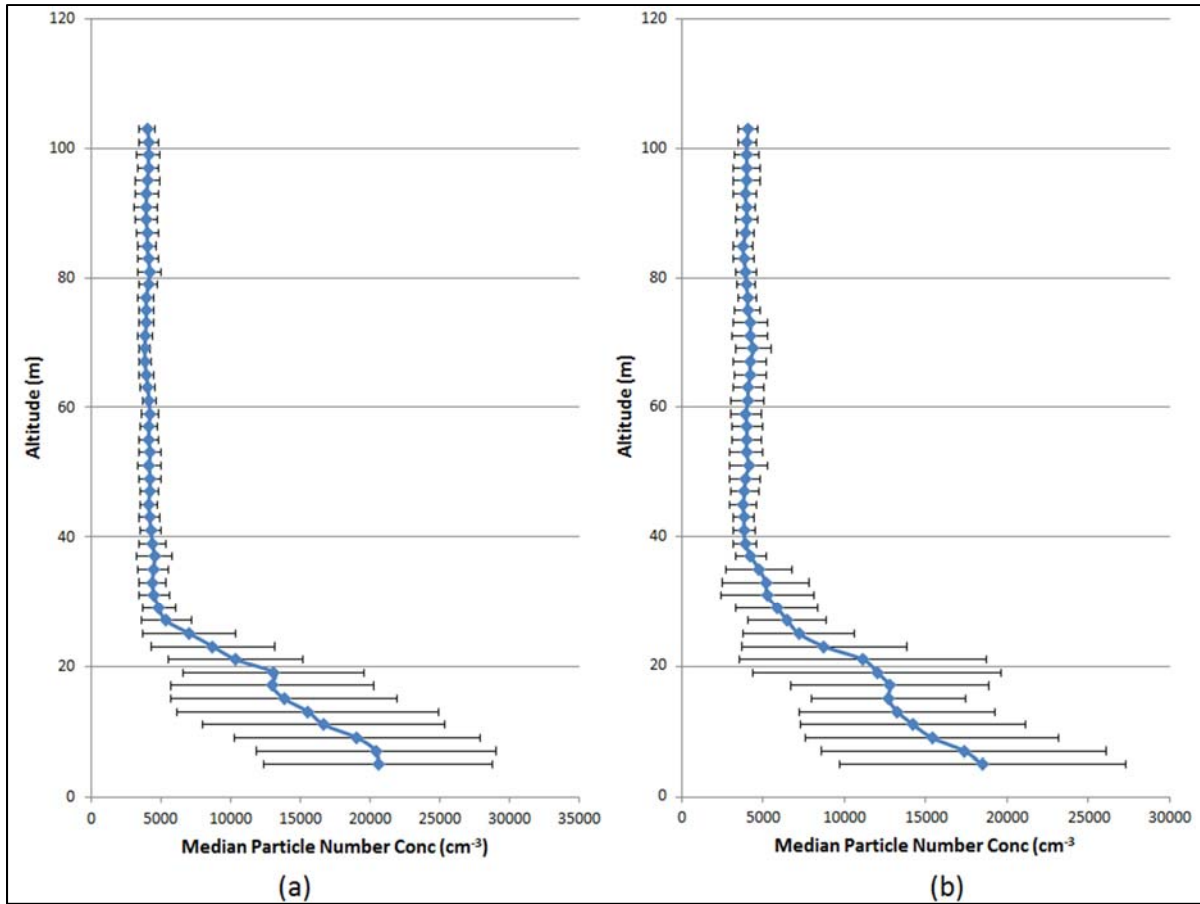
485

486 **Figure S3:** Aerial photo of the base camp and station

487

488

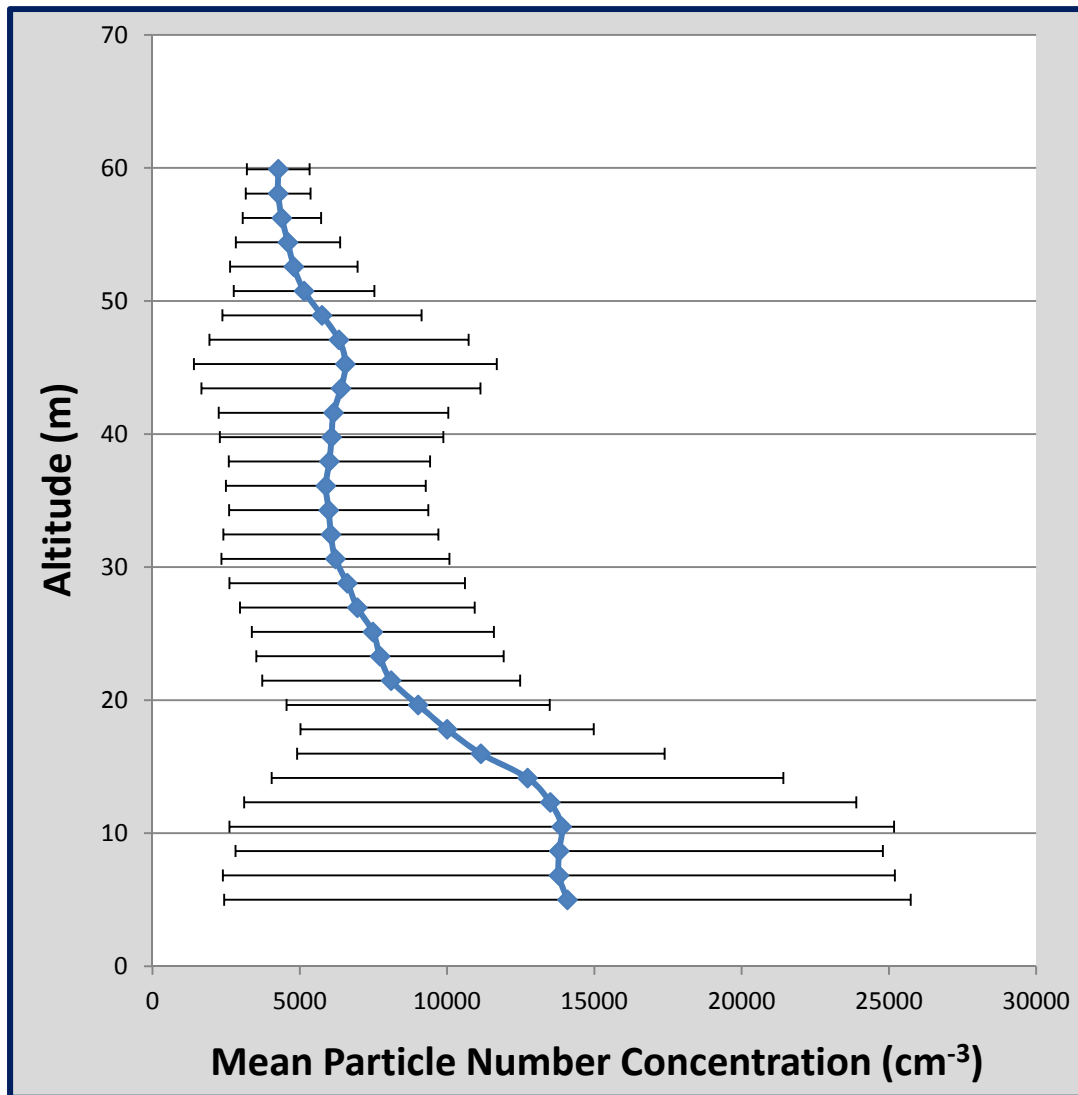
489



490

491 **Figure S4:** Means and standard deviations of the seven ascents (a) and descents (b) of the flights  
492 between 5 and 100 m.

493



494

495 **Figure S5:** PNC mean with standard deviation of both 12 ascends and 12 descents during the 5  
496 to 60 m vertical flights acquired during the optimization of the flight design.

497

498